Proceedings of ASME Turbo Expo 2011
GT2011
June 6-10, 2011, Vancouver, British Columbia, Canada

GT2011-45681

EXPERIMENTAL STUDY OF SIMULATED EFFECT OF ROTOR STATOR INTERACTION: EFFECT OF AXIAL SPACING AND ROTOR BLADE FILM COOLING AIR INJECTION RATIO

Murari Sridhar, B.V.S.S.S.Prasad and N.Sitaram

Thermal Turbomachines Laboratory, Department of Mechanical Engineering
Indian Institute of Technology Madras, Chennai –600036, India

ABSTRACT

The effect of inlet wake and air injection on blade surface temperature distribution is experimentally determined in the present paper. A flat plate with smoothly curved leading edge and a symmetric beveled trailing edge is used to produce inlet wake. Experiments are performed on a seven-airfoil linear cascade in a low speed wind tunnel at the chord Reynolds number of $5.3x10^5$. Three blades in the middle of the cascade are provided with multiple rows of air injection holes on both pressure surface and suction surface. The distance between the trailing edge of the wake plate and leading edge of the cascade blade is kept at three axial locations, i.e. 0.25, 0.35 and 0.5 (all measured in terms of percent blade chord), at seven transverse locations for each axial location. The detailed temperature distributions on the blade surface are measured using "T-Type" thermocouples connected to a data logger. The results are obtained in terms of film cooling effectiveness for a density ratio (between the hot fluid through air injection holes and cold main flow fluid) of 1.1 and injection mass flow rates of 1.1, 2.5, 3.0 and 5.0 percent of main flow. A significant change in the film cooling effectiveness is observed with increase in the injection mass flow rate and change in the axial spacing.

INTRODUCTION

The objective to improve a turbomachine in view of compactness and performance is always on a high with current interest being on the rotor-stator interaction of the fluid flow. The reduction of axial space between the blade stages lessens its aerothermal performance because of the effects of unsteadiness of wake caused by rotor and stator on each other. The mechanism of fluid flow through the discrete holes of the turbine and thus making a film cooling effect also affects the aerothermal performance of the blade. The interest on the rotor-stator interactions is mainly evolved in 1982 when Dring et al. [1] emphasized the difficulty in generalizing the optimum gap and its importance through his experimental investigation on a turbine stage at large scale rotating rig facility. Dunn et al. [2] studied the influence of vane/blade spacing (0.19% and 0.50% of rotor chord) on stage heat flux distributions and has observed that the rotor blade Stanton number is sensitive to the vane blade spacing. Abhari et al. [3] with a goal to quantify the impact of stator rotor interactions on film cooled blade have observed the uploading behavior on the injection regions of suction surface. No film effectiveness data is provided to understand the influence of such interaction effects on film cooling effectiveness. Venable et al. [4, 5] performed a comprehensive study to determine the influence of vane-blade spacing on transonic turbine stage aerodynamics. Unsteady pressure data are taken for three different vane-blade row spacing and results indicated that the magnitude of the surface pressure unsteadiness on the vane and blade changes significantly with vane-blade axial spacing. Later Dunn et al. [6] performed an experimental study to study the influence of vane/blade spacing on heat flux for transonic turbine by employing the fixed film injection ratio at three different axial spacing such as 20%, 40% and 60% of vane axial chord. It is noticed that the influence of vane/blade spacing on the blade heat loads is minimal. Denos et al. [7] presented experimental results of the unsteady flow through the rotor of a transonic turbine stage which emphasized the effects of variation of rotational speed of the rotor, the axial stator rotor spacing and stator trailing edge coolant flow injection and concluded that the increase in axial spacing from 35 percent to 50 percent of stator axial chord decreases the amplitude of the fluctuating rotor pressures. Yamada et al. [8] performed a similar study with three axial gaps being tested which are achieved by moving the stator vane in the axial direction while keeping the disk cavity constant. The effect of the axial gap is investigated

at design and off-design conditions and the linear improvement in turbine efficiency with the change in axial gap is noticed. Gaetini et al. [9] performed analysis on the unsteady flows in a low aspect-ratio turbine stage considering three vane rotor axial gaps ranging from 16% to 50% of stator axial chord and steady flow measurements at different locations in the stator-rotor gap are carried out to provide a complete description of the three dimensional flowfield entering the rotor. The blade row interaction and its dependence on the axial gap are evaluated by means of phase-resolved aerodynamic measurements at downstream of the rotor. The blade row interaction is mainly driven by the vortex-blade interaction in the hub region and by the unsteadiness of the incidence at rotor which is produced by the stator flow structures. The interaction phenomena vary with the variation of axial gap depending on the magnitude of the stator vortices and the superimposition between the stator wake and potential field.

Yamamoto et al. [10] studied the interaction of turbine stator and rotor using two linear cascades installed in series and by measuring total pressure losses at different locations at downstream the cascade. Their magnitudes are found to be maximum when the upstream cascade passes the suction side of the downstream passage. Du et al. [11] studied the effects of unsteady wake on the film cooling performance of a gas turbine blade which has the coolant ejection at the trailing edge. Usage of transient liquid crystal to measure surface distribution is employed and a good match with the author's similar previous investigation is found where thin foil thermocouples are used. It is justified that the unsteady wake helps to increase the inlet turbulence and hence the rotor surface heat transfer rate. Inlet wake along with the trailing edge jet when combined helps in providing enhanced heat transfer coefficient and early flow transition on blade suction surface. Prior to these investigations, in 1998, Sitaram et al. [12] studied the effect of inlet wake on total pressure loss of a linear turbine rotor cascade. It is reported that the lift coefficient depends on the position of wake generator. With a modification of the test facility used by them in terms of facilitating the film air to the cascades Sridhar et al. [13] performed experiments to study the influence of inlet wake and film air blowing ratio on static pressure distribution of turbine rotor cascade blade and noticed that the blade loading is strongly influenced by the axial gap and film air blowing ratio. All the above refereed experiments on typical turbine blade profiles were carried out in the Reynolds number range of $5x10^5$ to $7x10^5$. These Reynolds numbers are believed to simulate the wake effects and film cooling effects accurately.

From the above brief review it is clear that the reduction in axial spacing between the blade stage to make the turbine stage compact influences the aerodynamic and heat transfer performance due to change in the intensity of wakes generated by the upstream vane trailing edges. In continuation to the work done, the authors presented the effect of inlet wake and air injection on blade surface temperature distribution in the current paper. A flat plate with smoothly curved leading edge and a symmetric beveled trailing edge is used to produce inlet wake. Experiments are performed on a seven-airfoil linear cascade in a low speed wind tunnel at the chord Reynolds number of $5.3x10^5$. Three blades in the middle of the cascade are provided with multiple row air injection holes on both pressure surface and suction surface. The distance between the trailing edge of the wake plate and leading edge of the cascade blade was kept at three axial locations like 0.25, 0.35 and 0.5 (all measured in terms of percent blade chord), at seven transverse locations for each axial location. The detailed temperature distributions on the blade surface are measured using "T-Type" thermocouples connected to a data logger. The results are obtained in terms of film effectiveness for a density ratio (between the hot fluid through air injection holes and cold main flow fluid) of 1.1 and injection mass flow rates of 1.1, 2.5, 3.0 and 5.0 percent of main flow. A significant change in the film effectiveness is observed with increase in the blowing ratio and change in the axial spacing.

NOMENCLATURE

a	Axial chord (mm)
BR	Blowing ratio
Ch	Blade chord (mm)
d	Diameter of film hole pipe (mm)
L/d	Ratio of hole length to hole diameter
L	Length of film hole (mm)
p/d	Ratio of hole pitch to hole diameter
s	Axial distance from leading edge of blade
S	Blade spacing (mm)
$T_{surface}$	Blade surface temperature (^oC)
$T_{freestream}$	Free stream temperature (^oC)
$T_{injection\ air}$	Injection air temperature (^oC)
V_m	Velocity of film injection air (m/sec)
V_∞	Velocity of main stream fluid (m/sec)
WG	Wake generator
x	Axial distance between flat plate trailing edge and Leading edge of cascade (mm)
X	Non-Dimensional axial distance between flat plate trailing edge and leading edge of cascade blade (x/a)
y	Transverse distance between the flat plate trailing edge and leading edge of cascade blade.
Y	Non-Dimensional transverse distance between the flat plate trailing edge and leading edge of cascade blade (y/S)
η	Temperature effectiveness
ρ_m	Density of film air (kg/m^3)
ρ_∞	Density of main stream fluid (kg/m^3)
α_{film}	Angle between film hole axis and tangent of blade surface (Deg.)

Experimental facility

Linear cascade tunnel: The present experimental investigation is carried out in the low speed large cascade tunnel at the Thermal Turbomachines Laboratory of the Department of Mechanical Engineering at IIT Madras. The layout of the facility is shown in Figure 1. A centrifugal blower driven by a 75 kW D.Cmotor operating at a design speed of 1000 rpm delivers 14 m^3/s of air at 250 mm of water gauge to the tunnel. The motor speed can be continuously varied by changing the input voltage. More details of the facility, cascade along with the details of the wake generator (WG) are given by Sitaram et al. [12].

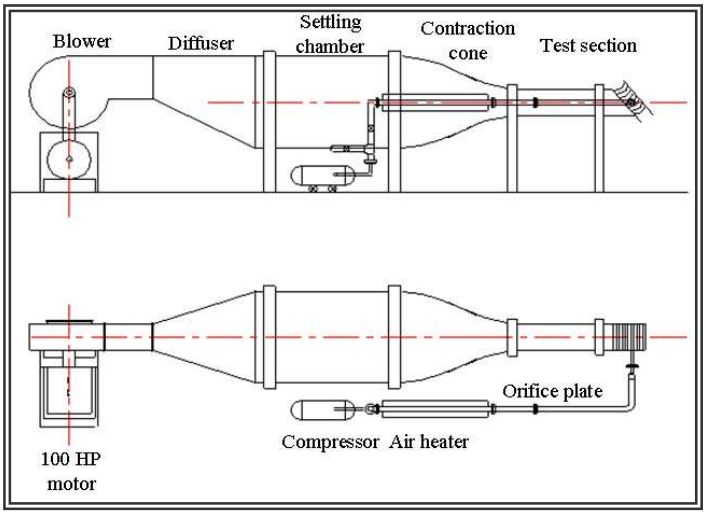

Fig. 1 Low speed cascade tunnel at IITM

A separate blower is used to deliver air continuously in to the plenum chambers provided for the middle three blades and thus through the injection holes provided on both pressure and suction surfaces of the blades. Flow rate of the injection fluid is controlled by properly bypassing the excess air through the bypass valve. In order to maintain a density ratio, the injection fluid is to be supplied at a different temperature than the free stream. To heat the injection fluid in the test facility, an electrical resistance heater is employed. This heater provides the injection air temperature rise of about 25 ^oC above the room temperature. A photograph of the film air supply layout is given in Figure 2.

Cascade: The blade profile used in the cascade is highly cambered with three rows of film holes on suction surface and two rows of film holes on pressure surface. The geometric details of the blade profile and cascade are provided in Figure 3 and the details of blade profile are provided in Table 1.

The experiments are conducted on this facility as the objective behind the test is to generate the test data. This data will be used by the authors to validate the computational studies which are planned to study the combined effect of axial gap and film air mixing on turbine aerodynamics and heat transfer. The middle three blades are fabricated out of aluminum sheets. Air injection holes are provided on the surface of these blades with three rows on suction surface and two rows pressure surface.

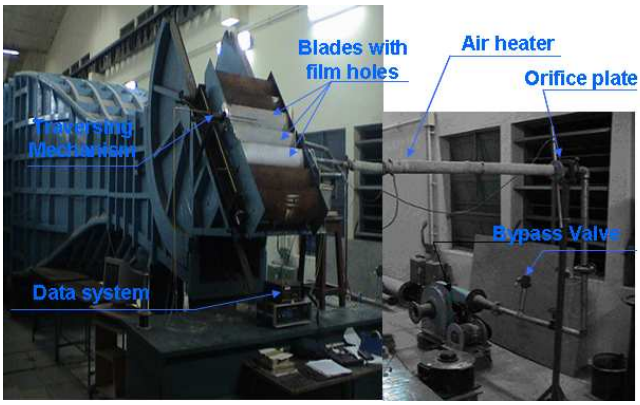

Fig. 2 Cascade tunnel with Film air supply system

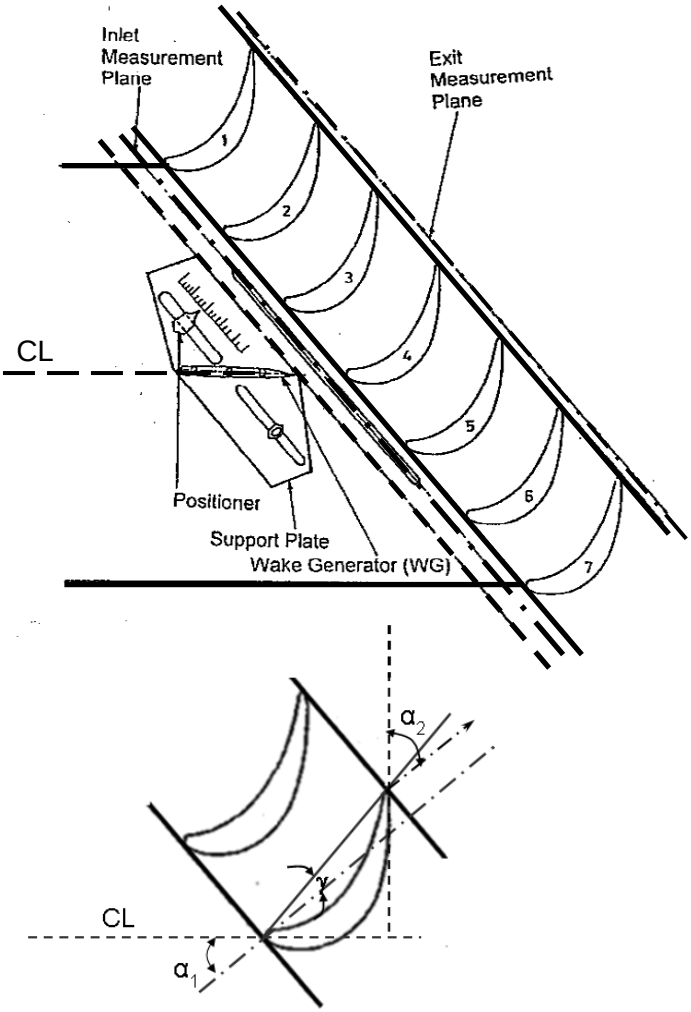

Fig. 3 Schematic of cascade with wake plate

Table 1: Blade profile specifications and coordinates

Blade profile specifications			
Blade chord, Ch	250 mm	Inlet blade angle, α_1	48°
Blade span, S	800 mm	Exit blade angle, α_2	52°
Space-chord ratio, S/Ch	0.65	Aspect ratio, AR	3.2
Maximum thickness, t_{max}/Ch	0.185	Stagger angle, γ	11°
Maximum camber position, a/Ch	0.4	Number of blades, N	7

Blade profile coordinates			
Suction surface		Pressure surface	
x (mm)	y (mm)	x (mm)	y (mm)
-3.33	5.65	6.40	1.08
-3.00	10.30	9.75	4.10
-1.50	17.80	14.70	9.30
0.70	25.50	19.65	14.70
3.45	33.45	24.85	20.13
10.30	48.85	35.27	29.98
20.16	64.35	46.36	39.13
51.20	91.70	70.38	52.81
94.75	103.90	96.40	57.90
134.50	97.60	123.20	56.10
164.90	81.40	150.35	50.65
189.70	61.50	177.60	41.90
211.00	40.88	203.27	30.37
231.90	21.00	226.88	15.07
242.90	11.20	238.06	6.27
Leading edge radius = 24% of t_{max}, Trailing edge radius = 12% of t_{max}			

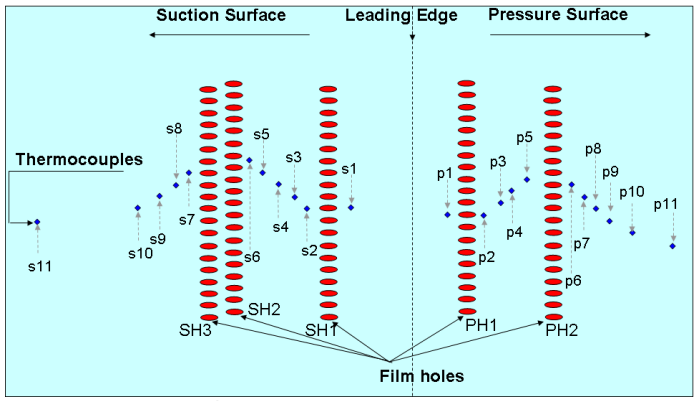

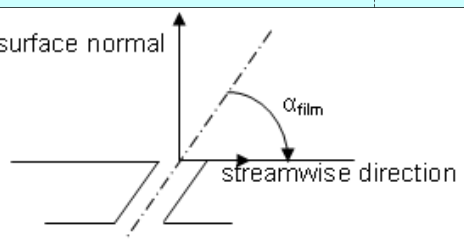

Fig. 4 Schematic of film-hole and thermocouple location

All the holes are in 1 mm diameter and are angled at 35 degrees to the blade surface. The holes are 3.5 mm long resulting in a length-to-diameter ratio (L/d) of 3.5. The pitch to diameter ratio (p/d) of the holes is maintained as 3. Schematic of film hole locations and thermocouple locations are shown in Figure 4.

The nondimensional surface distance of the film holes and thermocouples from the leading edge is provided in Table 2.

Table 2: Film hole and thermocouple location details

Location of filmholes on blade surface				
Film hole row	s/a	type	p/d	α_{film} (degrees)
SH1	0.100	cylindrical hole	3	35
SH2	0.140	cylindrical hole	3	35
SH3	0.152	cylindrical hole	3	35
PH1	0.150	cylindrical hole	3	35
PH2	0.380	cylindrical hole	3	35

Location of thermocouples on blade surface			
Thermocouple no.	s/a	Thermocouple no.	s/a
p1	0.100	s1	0.090
p2	0.140	s2	0.120
p3	0.160	s3	0.150
p4	0.180	s4	0.170
p5	0.210	s5	0.200
p6	0.280	s6	0.300
p7	0.390	s7	0.390
p8	0.410	s8	0.410
p9	0.500	s9	0.500
p10	0.600	s10	0.600
p11	0.900	s11	0.900

For the measurement of static pressure distribution the middle blade of the cascade is provided with static pressure taps. Steel tubes of 3 mm diameter are provided at various stations along the suction and pressure surfaces of the blade such that the tubes are flush with the blade profile. A hole of 0.6 mm diameter is drilled in these tubes to measure the surface static pressure distribution. Twenty-six and eighteen of such tubes to measure the static pressure are provided on the suction and pressure surfaces respectively. The details of the experimental investigations are provided in Table 3.

Table 3: Test details

s.no	X	Y	Blowing ratio
1	no wake plate		0, 0.8, 1.0, 1.2, 1.4
2	0.25	0.50, 0.25, 0.1, 0,- 0.1,-0.25 and- 0.5	0, 0.8, 1.0, 1.2, 1.4
3	0.35	0.50, 0.25, 0.1, 0,- 0.1,-0.25 and- 0.5	0, 0.8, 1.0, 1.2, 1.4
4	0.5	0.50, 0.25, 0.1, 0,- 0.1,-0.25 and- 0.5	0, 0.8, 1.0, 1.2, 1.4

Blowing ratio is defined as $BR = (\rho_m V_m) / (\rho_\infty V_\infty)$

Where ρ is density of the fluid, V is the velocity of the fluid, suffix 'm' represents injection fluid and '∞' for mainstream fluid. BR=0.0 corresponds to no fluid injection case. . Negative Y (y/S) means the WG is placed on the suction side of the instrument blade. When Y is positive, the WG is placed on the pressure surface side of the instrument blade and at zero Y, the WG is in line with the leading edge of the instrument blade.

To measure the blade surface temperatures T-Type (Copper/constantan) thermocouples are mounted on the blade surface. These thermocouples are recommended to measure the temperature in the range of -270 to 400 degree Celsius. In the measured range between 30 and 60 degree Celsius, the accuracy of measurement is about 0.25 degree, measured with the instrument resolution of 0.025 degree (~1μv). The thermocouples are precalibrated using a standard ASME [14] calibration procedure.

Instrumentation

The pressures from blade surface static pressure tubes are measured with a scanning box and micro manometer (± 200 mm range, ± 0.1 mm accuracy) manufactured by Furness Controls Ltd., Bexhill, London. An orifice plate which is fabricated as per ASME standards is used to find the flow rate of the injection fluid. Pressure taps are provided at a distance of one diameter and one-and-half diameter upstream and downstream of the orifice plate respectively to measure the pressure difference and thus velocity and mass flow rate are measured subsequently. Precalibrated five-hole probes are traversed at the inlet and exit of the cascade to check the periodicity of the cascade blade. Inlet measurements are made. at 15 percent chord upstream of the cascade blade and exit measurements are made at 10 percent chord downstream of cascade blade. The probe traverse is made at blade centre line where all the instrumentation is done. The calibration of five hole probe is made as per the ASME standards. Precalibrated T-type thermocouple is used to measure the temperature of the hot injection fluid. The thermocouple calibration is done as per the ASME standard procedure. The thus calibrated thermocouples are mounted on blade surface. The thermocouples are brazed to a copper plate and the same is flushed on the blade surface. After mounting of thermocouples, the surface of the blade is polished with fine graded emery papers, so that the surface is made free of surface burrs and roughness. Hence the thermocouples do not cause interference to the boundary layer.

Results and Discussion

Experiments are performed at a cascade inlet Reynolds number of 5.3×10^5. The corresponding flow velocity at cascade inlet is 20 m/s. Air as injection fluid is tested at blowing ratios of 0.0, 0.8, 1.0, 1.2 and 1.4 for without and with wake generator (WG): positioned from X=0.25 to 0.50 and Y = -0.5 to 0.5. For all cases, injection air temperature is maintained at 54°C. To validate the cascade periodicity arrangement, a five hole probe is traversed to cover the three cascade blades. Figure 5 shows the total pressure distribution at the exit traverse plane. Considering the experimental uncertainties which are of the order of ±5%, the periodicity observed in the experimental data is reasonable. Periodic repetition of the wake signifies the trueness in the cascade blade arrangement. A probe is traversed at the inlet traverse plane of the cascade to quantify the wake

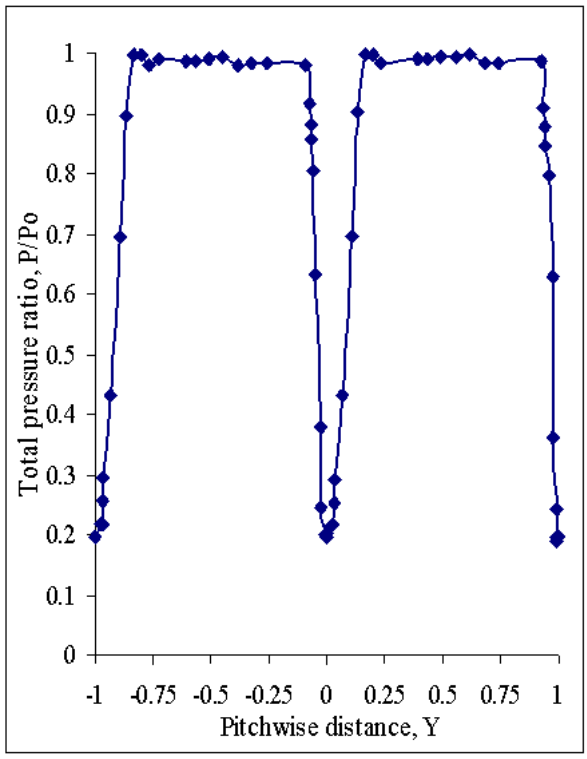

Fig. 5 Total pressure at exit traverse plane

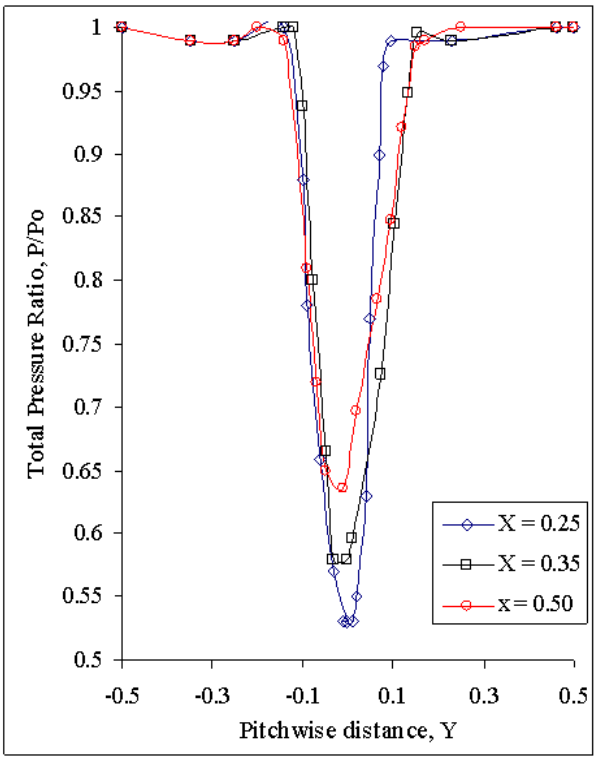

Fig. 6 Total pressure at inlet traverse plane

effect with respect to axial spacing. Total pressure variation at inlet traverse plane is plotted in Figure 6. Intensity of the wake

with respect to axial spacing is observed in terms of the magnitude of total pressure loss. The effect of blade axial spacing and blowing ratio on blade surface temperature distributions is assessed by studying the effectiveness distributions on blade surface. Effectiveness on blade surface is calculated as

$$\eta = (T_{surface} - T_{freestream})/(T_{injection\ air} - T_{freestream})$$

Effect of blowing ratio: Figure 7 presents the effect of blowing ratio on surface effectiveness distribution. The surface effectiveness is the non-dimensional representation of temperature distribution on blade surface.

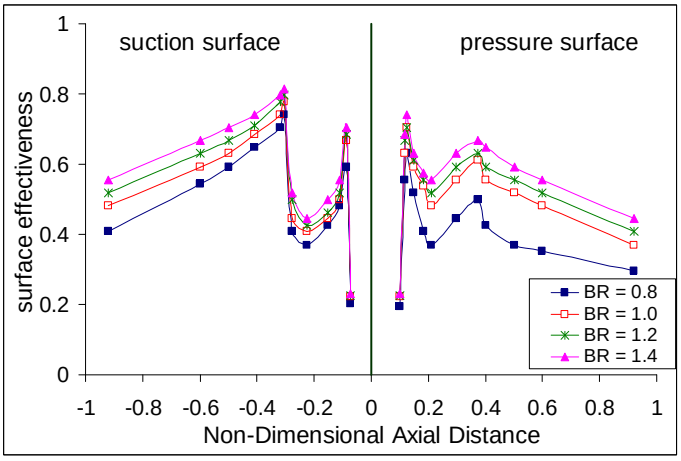

Fig. 7 Effect of blowing ratio

For an ideal film cooled turbine blade the effectiveness is expected to be unity. This signifies the 100% protected surface from hot mainflow gases. The viscous property of the fluid helps in generating the momentum boundary layer and thermal boundary layer which thus brings down the surface effectiveness. The peaks in surface effectiveness on both suction and pressure surfaces are due to better film coverage at downstream of the film holes. Followed by the peaks, the surface effectiveness decreases due to injection dilution. Injection dilution increases with the distance from the film holes. Ameri et al. [15] says that the better film coverage is due to three dimensional nature of the jet and gets diluted to two dimension far downstream at X/D>15. Injection dilution intensity is more on suction surface than pressure surface due to the acceleration of the fluid on the suction surface. Surface effectiveness increases with increase in the blowing ratio and the effect of blowing ratio on surface effectiveness is more predominant far downstream the film holes. This is due to the dilution of horse shoe vortex which is generated near the exit of film hole. This is explained by Leylek et al. [16] as jet lift-off .

Effect of inlet wake and blowing ratio: After understanding the effect of blowing ratio on the cascade blade surface effectiveness, further investigation is made to understand the effect of inlet wake and blowing ratio on the effectiveness.

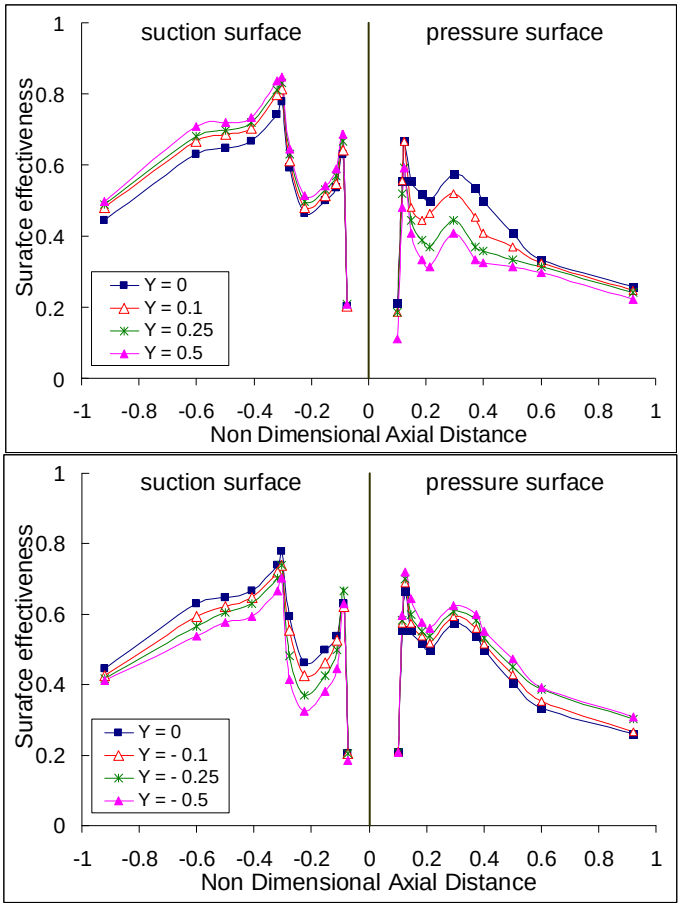

Fig. 8 Effectiveness on blade surface: WG at X=0.25, Y=–0.5 to 0.5, BR=0.8

Experiments are done for each blowing ratio (0.8, 1.0, 1.2 and 1.4) by changing the WG position both in axial and transverse directions. Required blowing ratio is maintained by properly controlling the injection fluid flow by means of a butterfly valve provided in the injection fluid passage. Temperature on the blade surface is measured for all the defined settings.

Figure 8 shows the effect of inlet wake and blowing ratio on effectiveness distributions on suction and pressure surfaces respectively when the WG is placed at X=0.25 and at BR of 0.8. The behavior of inlet wake on the suction surface of the blade is observed to be different from that of pressure surface. The effectiveness on the suction surface is minimum when the WG is located at Y=0. This is the position where the wake due to WG interacts with the LE of the cascade blade. The effectiveness increases when the WG is moved away towards the positive Y direction from the above mentioned location. With the intensity of wake being maximum at Y=0 location, it is understood that the intensity of wake decreases the surface effectiveness in the flow acceleration regions. On the pressure surface of the blade the effectiveness is maximum when the WG is positioned at Y=–0.5. This is the position where the WG

is placed at farthest location on suction surface. As the WG is moved towards the pressure surface, the effectiveness decreases.

Figures 9 shows the effectiveness distribution on blade surface with wake generator (WG) positioned at X=0.25 and a blowing ratio (BR) of 1.4.

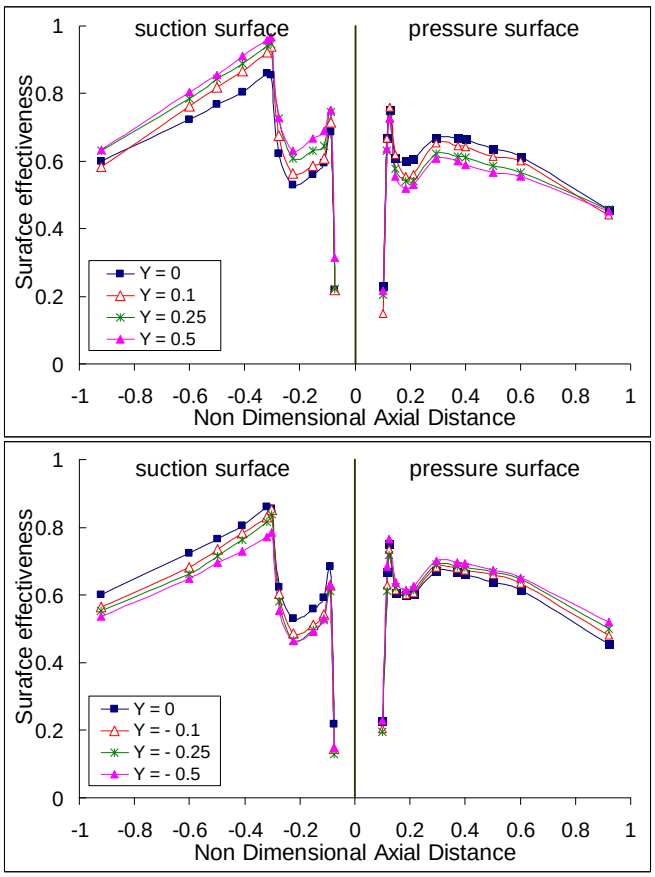

Fig. 9 Effectiveness on blade surface: WG at X=0.25, Y=–0.5 to 0.5, BR=1.4

On blade suction surface, the effectiveness distribution follow the similar trend as when BR=0.8. The maximum effectiveness is obtained when the WG plate is placed at Y=0.5. Suction surface of the blade experiences minimal Wake from WG at this position. Variation in the surface effectiveness, due to WG position, would get minimize as the Blowing ratio is increased from 0.8 to 1.4.

Similar to suction surface, the difference in the behavior of effectiveness on pressure surfaces at different Y positions minimizes when BR is increased from 0.8 to 1.4. The maximum effectiveness is obtained when the WG plate is placed at Y=–0.5 which is similar to X=0.25 and BR=0.8 case.

The behavior of surface effectiveness when the WG is moved from X=0.25 to 0.35 and with the blowing ratio maintained as 0.8 is shown in Figure 10. At the BR=0.8 and at X=0.35, the lateral spread of effectiveness with change in the transverse

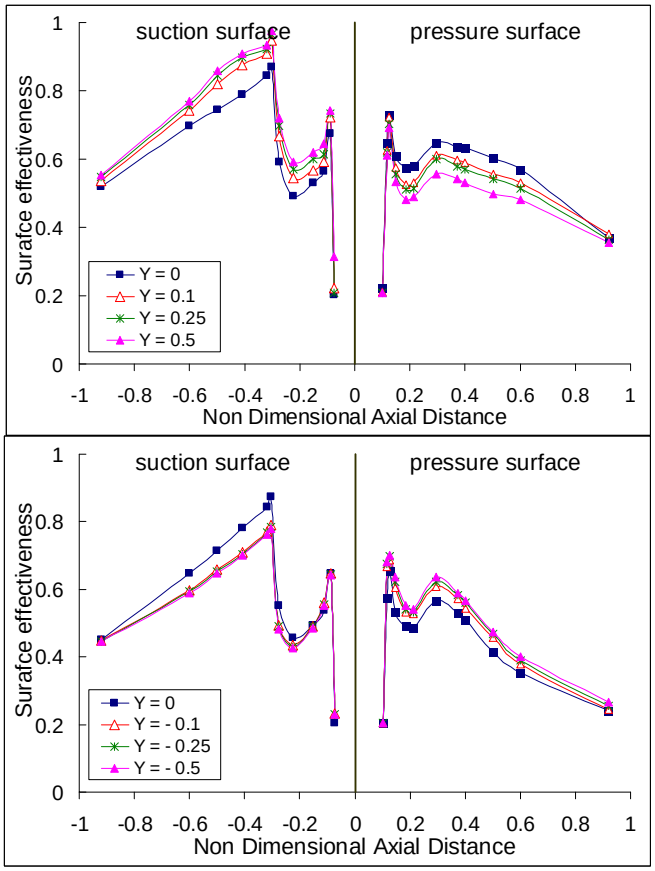

Fig. 10 Effectiveness on blade surface: WG at X=0.35, Y=–0.5 to 0.5, BR=1.4

position of wake decreases both on pressure surface and suction surface, compared to X=0.25 position.

Figure 11 shows the effectiveness distribution at X=0.35 and BR=1.4. Similar to low blowing ratio case, the lateral spread of effectiveness is minimized at BR=1.4.
Effectiveness distribution on blade surface when X=0.35 and BR=1 and 1.2 follow the similar trend to that of BR = 1.4 and so the plots were not provided here. However the data is taken in to consideration while interpreting the overall behaviour of wake with different WG locations in X and Y directions.

Figures 12 and 13 show the effect of WG when located at X=0.5 and at BR=0.8 and 1.4, on surface effectiveness. As the inlet wake intensity is reduced by moving the WG from X=0.25 to X=0.5 the effect of inlet wake on surface effectiveness reduces. The effectiveness curves moves close to no WG case. The effect of inlet wake on pressure surface is observed for all WG positions on pressure surface when the BR is 0.8. This signifies that when the film velocity is less than the main stream velocity the influence of wake is experienced on pressure surface irrespective of WG positions.

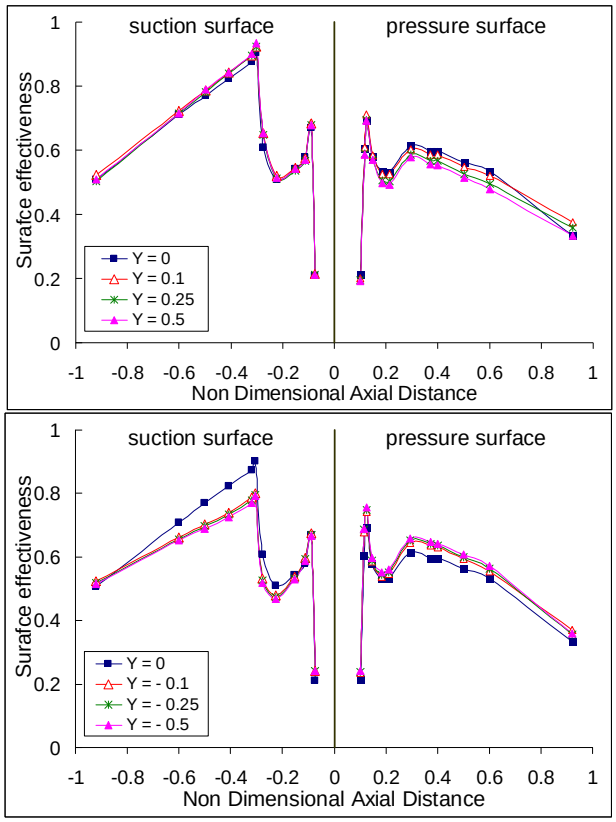

Fig. 11 Effectiveness on blade surface: WG at X=0.35, Y=–0.5 to 0.5, BR=1.4

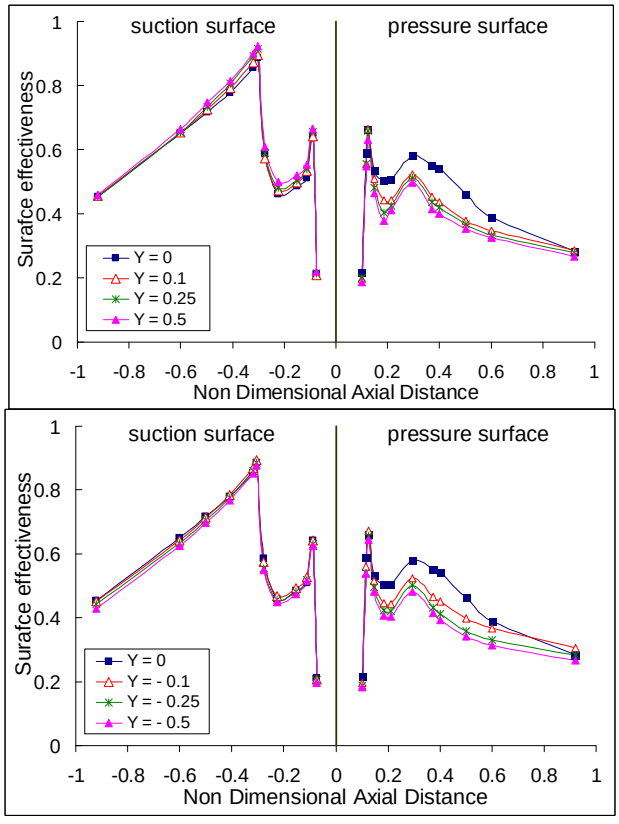

Fig. 12 Effectiveness on blade surface: WG at X=0.50, Y=–0.5 to 0.5, BR=0.8

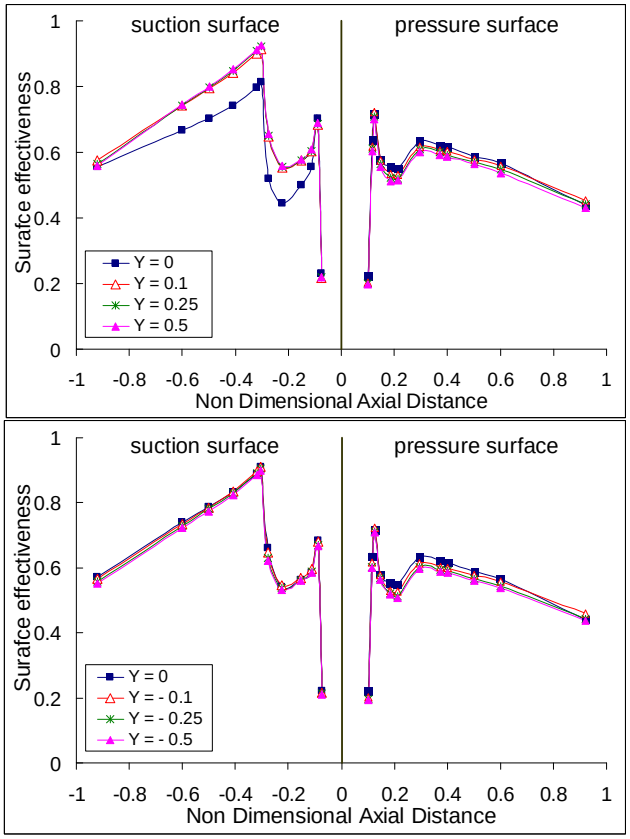

Fig. 13 Effectiveness on blade surface: WG at X=0.50, Y=–0.5 to 0.5, BR=1.4

To have a clear understanding of the effect of wake and blowing ratio on surface effectiveness distribution, the data obtained at all WG locations and BR are area averaged.

Figure 14 provides an overall idea on the effect of inlet wake and BR on surface effectiveness at axial spacing of 0.25. Effectiveness on the suction surface is higher than on the pressure surface. This is due to the reason that for the same plenum pressure, the pressure difference between the free stream air and the plenum air is more on suction surface and so the coolant flow is more spread on suction surface. Increase in effectiveness with blowing ratio is observed both on pressure surface and suction surface. Increase of slope of effectiveness curve on suction surface and decrease in slope on pressure surface signifies that the presence of wake decrease the effectiveness on the blade surface. Figure 15 shows the effectiveness variation when the wake plate is moved from 0.25 to 0.35. The effect of blowing ratio is reduced here. Similar behaviour of effectiveness variation with transverse position of wake plate is observed. Figure 16 shows effectiveness variation at wake plate position of 0.50. As the wake plate is moved away from the LE of cascade blade the effectiveness variation on blade surface is with the wake plate transverse position is minimized. This says that the influence of wake shedding has a positive effect on the blade surface effectiveness.

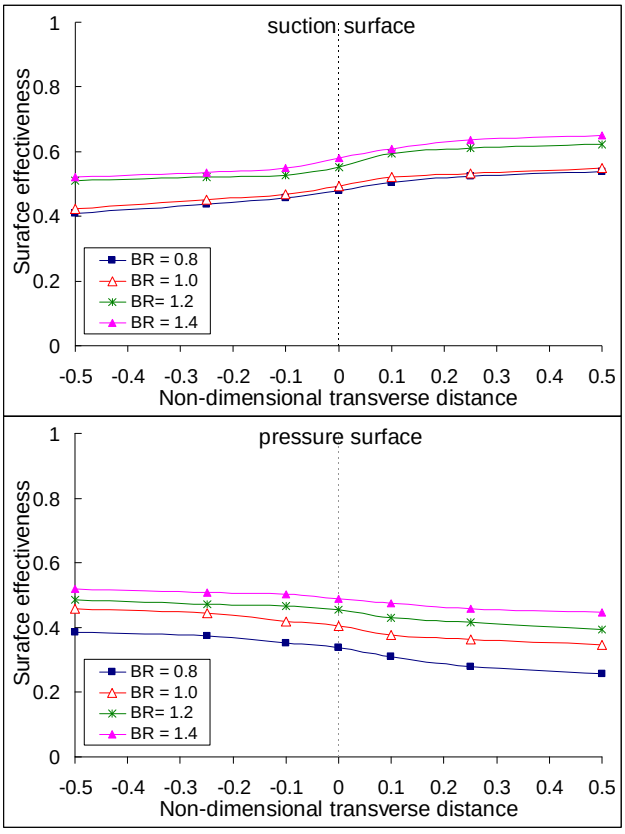

Fig. 14 Area averaged effectiveness at X=0.25

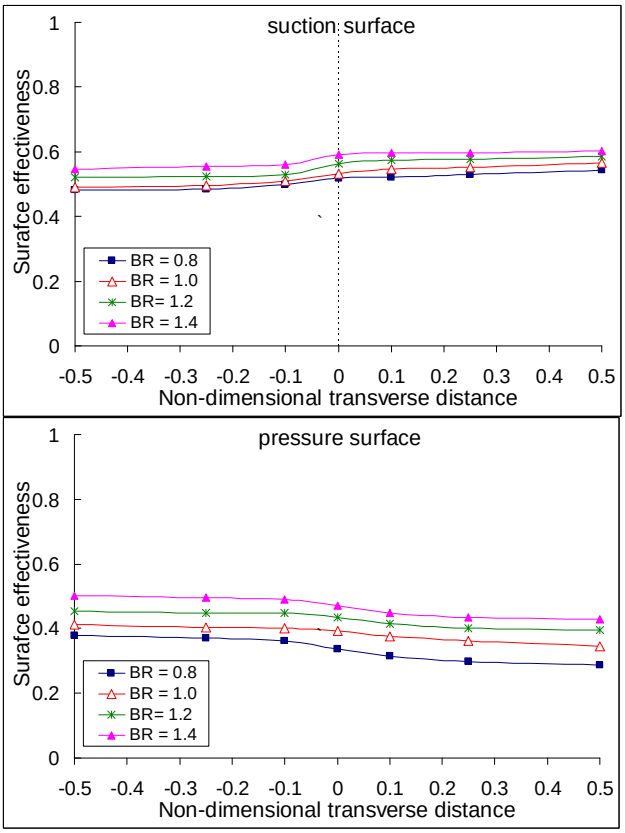

Fig. 15 Area averaged effectiveness at X=0.35

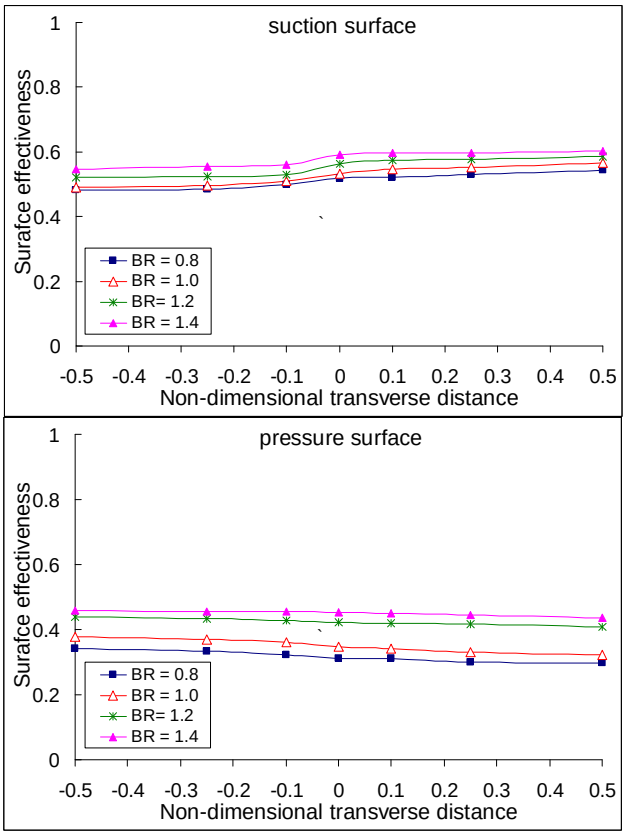

Fig. 16 Area averaged effectiveness at X=0.50

To quantify the effect of inlet wake on blade film effectiveness, the data at 0.25, 0.35 and 0.5 positions is mass averaged.

Figures 17(a) and 17(b) shows the mass weighted average effectiveness on suction and pressure surfaces of the blade with blowing ratio and with the variation in axial gap between the wake plate and cascade blade. For all the blowing ratios considered, the effectiveness is more on the suction surface when compare to pressure surface.

Effect of wake is seen in terms of decrease in the effectiveness on blade surface. The maximum effectiveness values are seen in the absence of wake plate. The effectiveness is minimized on suction surface when the wake plate is at the closest position. This behaviour is not seen on the pressure surface. Axial spacing of X=0.35 gives optimum overall surface effectiveness. From earlier investigation [13], maximum lift coefficient and minimum loss coefficient are obtained at this axial spacing. Hence for this configuration X=0.35 may be considered optimum from aerodynamic and heat transfer aspects.

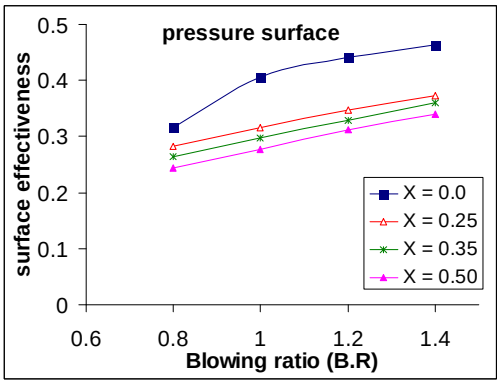

(a) mass weighted effectiveness on suction surface

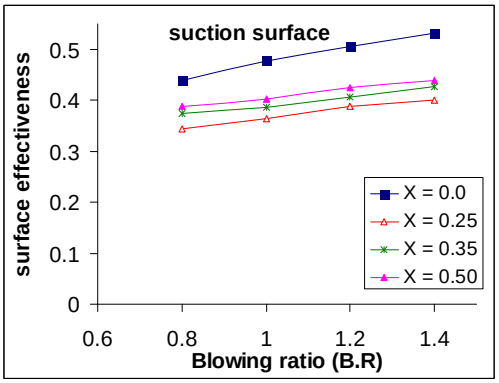

(b) mass weighted effectiveness on pressure surface

Fig. 17 Mass weighted average effectiveness

CONCLUSIONS

An experimental study is carried out to investigate the effect of inlet wake and air injection on blade surface temperature distribution. The non dimensional form of temperature called as temperature effectiveness is used to quantify for different axial spacings and blowing ratios. Based on the present study the following conclusions are drawn.

- Effectiveness increases with increase in the blowing ratio in the absence of inlet wake.
- For all the blowing ratios considered, the effectiveness is more on the suction surface when compared to pressure surface.
- At a given axial spacing the effectiveness is influenced with the transverse position of the wake plate.
- The magnitude of the influence of effectiveness on transverse location of wake plate decreases with increase in axial gap.
- Overall Effect of wake is seen in terms of decrease in the effectiveness on blade surface.
- For the axial spacing considered for investigation i.e., X = 0.35 gives optimum overall surface effectiveness.

REFERENCES

[1] Dring, R.P., Joslyn, H.D., Hardin, L.W., Wagner, J.H., 1982, "Turbine rotor-stator interactions", ASME J. Engg. Power, **104**(4) 729–740.

[2] Dunn, M.G., Chupp, R.E., 1989, "influence of vane/blade spacing and injection on stage heat flux distributions", AIAA J. Propulsion and Power, **5**(1) 212–220.

[3] Abhari, R.S., 1996, "Impact of rotor-stator interactions on turbine blade film cooling", ASME J. Turbo., **118**(1) 123–133.

[4] Venable, B.L., Delaney, R.A., Busby, J.A., Davis, R.L., Dorney, D.J., Dunn, M.G., Haldeman, C.W., Abhari, R.S., 1999, "Influence of vane-blade spacing on transonic turbine stage aerodynamics: Part I–Time averaged data and analyses", ASME J. Turbo., **121**(3) 663–672.

[5] Busby, J.A., Davis, R.L., Dorney, D.J., Dunn, M.G., Haldeman, C.W., Abhari, R.S., Venable, B.L., Delaney, R.A., 1999, "Influence of vane-blade spacing on transonic turbine stage aerodynamics: Part II –Time resolved data and analyses", ASME J. Turbo., **121**(3) 673–682.

[6] Dunn, M.G., Haldeman, C.W., Abhari, R.S., McMillan, M.L., 2000, "Influence of vane/blade spacing on heat flux for a transonic turbine", ASME J. Turbo., **122**(3) 684–691.

[7] Denos, R., Arts, T., Paniagua, G., Michelassi, V., Martelli, F., 2001, "Investigation of unsteady rotor aerodynamics in a transonic turbine stage", ASME J. Turbo., **123**(1) 81–89.

[8] Yamada, K., Funazaki, K., Kikuchi, M., Sato, H., 2009, "Influences of Axial Gap Between Blade Rows on Secondary Flows and Aerodynamic Performance in a Turbine Stage", ASME Paper GT2009–59855.

[9] Gaetani, P., Persico, G., Osnaghi, C., 2010, "Effects of axial gap on the vane-rotor interaction in a low aspect ratio turbine stage", AIAA J. Propulsion and Power, **26**(2) 325–335.

[10] Yamamoto, A., Murao, R., Suzuki, Y., Aoi, Y., 1995, "A Quasi-Unsteady Study on Wake Interaction Turbine Stator and Rotor cascades", ASME J. Turbo., **117**(3) 553–561.

[11] Du, H., Ekkad, S., Han, J.C., 1997, "Effect of unsteady wake with trailing edge coolant ejection on detailed heat transfer coefficient distributions for a gas turbine blade", ASME J. Turbo., **119**(2) 242–248.

[12] Sitaram, N., Parida, S.K., Prasad.B.V.S.S.S., 1998, "Effect of inlet wake on total pressure loss of a linear turbine rotor cascade", AIAA Paper 98–3576.

[13] Murari, Sridhar., Prasad, B.V.S.S.S., Sitaram,N., 2004, "Effect of inlet wake and blowing ratio on static pressure distribution of a turbine rotor linear cascade", Proc. of Seventh National Conference on Air Breathing Engines and Aerospace propulsion, NCABE2004, 658–673

[14] ASME Power Test code 19.3-1974, Temperature measurement.

[15] Ameri, A.A., Rigby, D.L., Heidmann, J.D., 2000, "A three dimensional coupled internal/external simulation of a film cooled turbine vane", ASME J. Turbo., **122**(2) 348–359.

[16] Leylek, J.H., Walters, D.K., 2000, "Impact of film cooling jets on turbine aerodynamic losses", ASME J. Turbo., **122**(3) 537–545.